Nuclear Engineering and Technology 52 (2020) 863–868

Contents lists available at ScienceDirect

Nuclear Engineering and Technology

journal homepage: www.elsevier.com/locate/net

Technical Note

Current compensation for material consumption of cobalt self-powered neutron detector

Xinxin Liu [a,*], Zhongwei Wang [a], Qingmin Zhang [b], Bangjie Deng [b], Yaobin Niu [a]

[a] College of Aerospace Science and Technology, National University of Defense Technology, Changsha, 410073, China
[b] Department of Nuclear Science and Technology, School of Energy and Power Engineering, Xi'an Jiaotong University, Xi'an, 710049, China

ARTICLE INFO

Article history:
Received 12 March 2019
Received in revised form
29 May 2019
Accepted 19 September 2019
Available online 21 September 2019

Keywords:
Self-powered neutron detector
Material consumption
De-convolution model

ABSTRACT

Co Self-Powered Neutron Detector (SPND) is confronted with the problem of material consumption, which causes the response current can neither reflect the change of neutron flux in time nor be proportional to the neutron flux. In this paper, a deconvolution-based method is established to solve this problem. First of all, a step signal of neutron flux is taken as an example to analyze its performance. When the material consumption of Co SPND is 10%, after compensation, the response current can be in correspondence of neutron flux. Finally, the effects of this model in different Signal-to-Noise Ratio are analyzed, which fully confirms the truth of its excellent performance for compensating Co SPND's signal.

1. Introduction

Self-Powered Neutron Detector (SPND) has the advantages of simple structure, no need of external power supply, tiny volume [1,2], etc. It has been extensively used to obtain the neutron flux in rigorous environment (heavy pressure, mega temperature and intense radiation) of nuclear reactor, especially in high neutron flux environment [3,4]. The typical emitter materials of SPND are ^{103}Rh, ^{59}Co and ^{51}V. In most references, they hold the view that the currents produced by Rh and V SPND include delayed part but the currents produced by Co SPND are prompt [5]. However, as Co SPND's material consumption increases, more and more ^{60}Co nucleus are produced by ^{60m}Co decay and ^{59}Co (n, γ) reaction [6]. Due to the ^{60}Co nucleus and the ^{61}Co nucleus produced by ^{60}Co (n, γ) reaction decaying with certain decay constants λ_{60} and λ_{61} respectively, the background current (generated by ^{60}Co decay) and a little delayed current (generated by ^{61}Co decay) are produced [7]. It causes the response current can neither reflect the change of neutron flux in time nor be in corresponding with neutron flux.

In order to decrease the delay time, a lot of methods were proposed. The complex operation by Laplace transformation and z transformation could effectively improve the real-time performance of SPND [8]. The robust filtering method could greatly decrease the delay time of SPND [9]. Besides, the dynamic compensation based on Kalman filter could also be very suitable for Co SPND [10]. In these references, the best result was that they optimized the delay time to be about 1 s, but it still could not reflect the real-time neutron flux. Recently, a deconvolution-based method was proposed to solve the problem of delayed current, however, it only analyzed the performance when the sampling interval was 0.1 s and they did not give a reasonable method to solve the problem of SPND's material consumption [11].

Therefore, a modified model based on de-convolution method [11] is established in this paper. After compensation, the problem caused by material consumption can be solved appropriately. The compensated current can not only reflect the change of neutron flux in time, but also be proportional to neutron flux.

2. Model establishment

2.1. Physical description

Cobalt SPND is extensively used in nuclear reactor protection system due to its excellent performance in high proportion of prompt current. However, as the consumption of emitter material ^{59}Co, many ^{60}Co nucleus are produced, which results in the depravation of its performance. It has serious impact on nuclear reactor's safety. So, a model based on a deconvolution method is established to solve this problem.

The interaction process between neutron and Co SPND is shown in Fig. 1 [12]. Neutrons interact with ^{59}Co nucleus to produce ^{60}Co

* Corresponding author.
E-mail address: lxx975716738@stu.xjtu.edu.cn (X. Liu).

https://doi.org/10.1016/j.net.2019.09.010

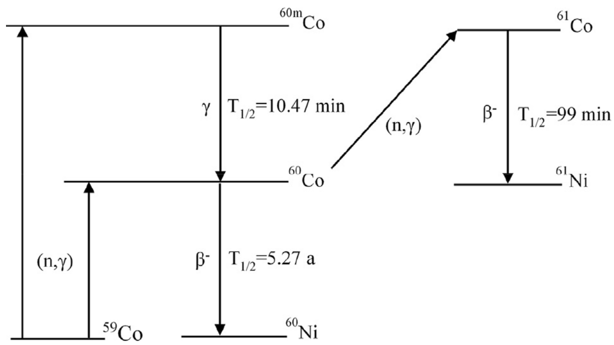

Fig. 1. The interaction process between neutron and Co SPND.

nucleus and ^{60m}Co nucleus, and γ rays are released in the meanwhile. Then ^{60m}Co nucleus decay to ^{60}Co nucleus with decay constant λ_{60m}, and ^{60}Co nucleus decay to ^{60}Ni nucleus with decay constant λ_{60}, while γ and β rays are released in these processes. At the same time, neutrons can also interact with ^{60}Co nucleus to produce ^{61}Co nucleus and release γ rays. After that, the ^{61}Co nucleus decay to ^{61}Ni with the decay constant λ_{61}, while γ and β rays can also be released.

The γ rays produced by the processes above can interact with the materials in Co SPND by photoelectric effect, Compton effect and electron pair effect to produce electrons. And then the electrons interact further with the materials in the detector by ionization and excitation to produce more electrons. When the electrons generated in the emitter and insulator are collected by the collector, the current can be obtained [13,14]. The definition and value of each variable and parameter are listed in Table 1 and Table 2.

Due to new Co SPND's material consumption can be ignored, the atomic density of ^{60}Co can be considered as 0. Therefore, the current can be described as follow.

$$I(t) = (f_{59g}\sigma_{59g} + f_{59m}\sigma_{59m})N_{59}(t)\Phi(t) + k_{60m}\lambda_{60m}N_{60m}(t) \tag{1}$$

Because the energy of γ rays generated by the process of ^{60m}Co nucleus decaying to ^{60}Co nucleus is very small (58.6 keV) and it cannot produce effective electrons to arrive the collector according by the experiment [15], the value of the current sensitivity coefficient k_{60m} can be assigned as 0. So, the current only contains prompt component and it is rewritten in Eq. (2).

$$I(t) = (f_{59g}\sigma_{59g} + f_{59m}\sigma_{59m})N_{59}(t)\Phi(t) \tag{2}$$

But when Co SPND has been used for a long time, the material consumption cannot be ignored. Its currents contain prompt component and delayed component. The prompt current is generated by ^{59}Co (n, γ) ^{60}Co reaction and ^{60}Co (n, γ) ^{61}Co reaction, while the delayed current is generated by ^{60m}Co nucleus decay, ^{60}Co nucleus decay and ^{61}Co nucleus decay. So, the Co SPND's currents can be given as follow.

$$I(t) = (f_{59g}\sigma_{59g} + f_{59m}\sigma_{59m})N_{59}(t)\Phi(t) + k_{60m}\lambda_{60m}N_{60m}(t) + f_{60}\sigma_{60}N_{60}(t)\Phi(t) + k_{60}\lambda_{60}N_{60}(t) + k_{61}\lambda_{61}N_{61}(t) \tag{3}$$

In which the physical model of atomic density can be given by the following equations [16]:

$$\frac{dN_{59}(t)}{dt} = -(\sigma_{59g} + \sigma_{59m})N_{59}(t)\Phi(t) \tag{4}$$

$$\frac{dN_{60m}(t)}{dt} = \sigma_{59m}N_{59}(t)\Phi(t) - \lambda_{60m}N_{60m}(t) \tag{5}$$

Table 1
The definition of each variable.

Variable	Definition	Units
$I(t)$	Co SPND's current	A
$\Phi(t)$	neutron flux	$n\cdot cm^{-2}\cdot s^{-1}$
$N_{59}(t)$	atomic density of ^{59}Co	$n\cdot cm^{-3}$
$N_{60m}(t)$	atomic density of ^{60m}Co	$n\cdot cm^{-3}$
$N_{60}(t)$	atomic density of ^{60}Co	$n\cdot cm^{-3}$
$N_{61}(t)$	atomic density of ^{61}Co	$n\cdot cm^{-3}$

$$\frac{dN_{60}(t)}{dt} = \sigma_{59g}N_{59}(t)\Phi(t) + \lambda_{60m}N_{60m}(t) - \lambda_{60}N_{60}(t) - \sigma_{60}N_{60}(t)\Phi(t) \tag{6}$$

$$\frac{dN_{61}(t)}{dt} = \sigma_{60}N_{60}(t)\Phi(t) - \lambda_{61}N_{61}(t) \tag{7}$$

Due to the variation of atomic density of ^{59}Co and ^{60}Co during a short measurement period can be neglected, it's supposed that both N_{59} and N_{60} are constant during this compensation process. Besides, due to the γ rays generated by ^{60m}Co nucleus decaying to ^{60}Co nucleus cannot produces effective electrons to arrive the collector, the value of k_{60m} can still be assigned as 0. Therefore, the equations above can be rewritten as follows, where the current coefficient for ^{59}Co (n, γ) reaction to neutron flux can be simplified as S_{59}=($f_{59g}\sigma_{59g} + f_{59m}\sigma_{59m}$)$N_{59}$ and the current coefficient for ^{60}Co (n, γ) reaction to neutron flux can be simplified as $S_{60} = f_{60}\sigma_{60}N_{60}$.

$$I(t) = S_{59}\Phi(t) + S_{60}\Phi(t) + k_{60}\lambda_{60}N_{60} + k_{61}\lambda_{61}N_{61}(t) \tag{8}$$

2.2. The unit impulse response of neutron flux

In the following analysis process, the current generated by ^{60}Co decay is regarded as background current and the current generated by ^{61}Co decay is regarded as delayed current. When different neutron flux interacts with Co SPND, different current can be generated. To establish the convolution relationship between $I(t)$ and $\Phi(t)$, Eq. (8) can be written as follow.

$$I(t) = \Phi(t)*h(t) + k_{60}\lambda_{60}N_{60} \tag{9}$$

Where $h(t)$ means the unit impulse response of neutron flux. In order to obtain the expression of $h(t)$, it's assumed that $\Phi(t)$ can be expressed by Eq. (10).

$$\Phi(t) = \delta(t) = \begin{cases} \infty(t=0) \\ 0(t\neq 0) \end{cases} \tag{10}$$

Considering Eq. (8) and Eq. (9), the expression of $h(t)$ can be written in Eq. (11).

$$h(t) = \Phi(t)*h(t) = I(t) - k_{60}\lambda_{60}N_{60} = \begin{cases} S_{59}\delta(t) + S_{60}\delta(t)(t=0) \\ k_{61}\lambda_{61}N_{61}(t)(t>0) \end{cases} \tag{11}$$

According to Eq. (7) and Eq. (10), the equation and initial condition about $N_{61}(t)$ can be written in Eq. (12).

$$\frac{dN_{61}(t)}{dt} = -\lambda_{61}N_{61}(t) \quad (t>0) \qquad N_{61}(0) = \int_{0^-}^{0^+} \sigma_{60}N_{60}\phi(t)dt = \sigma_{60}N_{60} \tag{12}$$

And then $N_{61}(t)$ can be expressed in Eq. (13).

Table 2
The definition of each parameter.

Parameter	Definition	Value and Units
σ_{59g}	microscopic absorption cross section of thermal neutron for ^{59}Co (n, γ) ^{60}Co reaction	37.17×10^{-24} cm^2
σ_{59m}	microscopic absorption cross section of thermal neutron for ^{59}Co (n, γ) ^{60m}Co reaction	20×10^{-24} cm^2
σ_{60}	microscopic absorption cross section of thermal neutron for ^{60}Co (n, γ) ^{61}Co reaction	2×10^{-24} cm^2
f_{59g}	current sensitivity coefficient for ^{59}Co (n, γ) ^{60}Co reaction	⁄(A·cm^3·s)
f_{59m}	current sensitivity coefficient for ^{59}Co (n, γ) ^{60m}Co reaction	⁄(A·cm^3·s)
f_{60}	current sensitivity coefficient for ^{60}Co (n, γ) ^{61}Co reaction	⁄(A·cm^3·s)
k_{60m}	current sensitivity coefficient for ^{60m}Co decaying to ^{60}Co	⁄(A·cm^3·s)
k_{60}	current sensitivity coefficient for ^{60}Co decaying to ^{60}Ni	⁄(A·cm^3·s)
k_{61}	current sensitivity coefficient for ^{61}Co decaying to ^{61}Ni	⁄(A·cm^3·s)
λ_{60m}	decay constant of ^{60m}Co	1.1035×10^{-3} s^{-1}
λ_{60}	decay constant of ^{60}Co	4.1682×10^{-9} s^{-1}
λ_{61}	decay constant of ^{61}Co	1.1667×10^{-4} s^{-1}

$$N_{61}(t) = \sigma_{60}N_{60}e^{-\lambda_{61}t} \tag{13}$$

Combining with Eq. (11), the expression of $h(t)$ can be obtained in Eq. (14).

$$h(t) = \begin{cases} S_{59}\delta(t) + S_{60}\delta(t)(t=0) \\ k_{61}\lambda_{61}\sigma_{60}N_{60}e^{-\lambda_{61}t}(t>0) \end{cases} \tag{14}$$

2.3. De-convolution model

When the neutron flux $\Phi(t)$ is arbitrary value, the total current can be defined in Eq. (15). In which, the delayed component generated by ^{61}Co nucleus decay can be defined in Eq. (16).

$$I(t) = \Phi(t)*h(t) + k_{60}\lambda_{60}N_{60} = S_{59}\Phi(t) + S_{60}\Phi(t) + \Phi(t)*h_{61}(t) + k_{60}\lambda_{60}N_{60} \tag{15}$$

$$I_{61}(t) = \Phi(t)*h_{61}(t) \quad h_{61}(t) = k_{61}\lambda_{61}\sigma_{60}N_{60}e^{-\lambda_{61}t}(t>0) \tag{16}$$

In order to eliminate the influence of delayed current and background current, a de-convolution model is established. First of all, the parameters are made discrete as follows. In which, n is the nth sampling point and Δt is the sampling interval.

$$\begin{cases} I'(n) = I(n\Delta t) \\ \Phi'(n) = \Phi(n\Delta t) \\ h'_{61}(n) = \int_{(n-1)\Delta t}^{n\Delta t} h_{61}(\tau)d\tau \\ I'_{61}(n) = I_{61}(n\Delta t) \end{cases} \tag{17}$$

After discretization, the value of the original parameter in the moment $n\Delta t$ is assigned to the new parameter in the nth sampling point. Then the total current in the (n+1)th sampling point can be obtained in Eq. (18).

$$I'(n+1) = (S_{59}+S_{60})\Phi'(n+1) + \sum_{i=1}^{n}\Phi'(i)h'_{61}(n+1-i) + k_{60}\lambda_{60}N_{60} \tag{18}$$

In which, the delayed component of unit impulse response current can be derived from Eq. (16) and Eq. (17), which finally can be described in Eq. (19).

$$\begin{cases} h'_{61}(1) = k_{61}\sigma_{60}N_{60}(1-e^{-\lambda_{61}\Delta t}) \\ h'_{61}(n+1) = h'_{61}(n)e^{-\lambda_{61}\Delta t}(n \geq 1) \end{cases} \tag{19}$$

Then the expressions of delayed current in arbitrary neutron flux can be obtained in Eq. (20). In order to accommodate the need of calculation, it's assumed that the initial conditions $I'_{61}(0) = 0$ are reasonable when Co SPND is a new detector.

$$I'_{61}(n+1) = \sum_{i=1}^{n}\Phi'(i)h'_{61}(n+1-i) = I'_{61}(n)e^{-\lambda_{61}\Delta t} + \Phi'(n)h'_{61}(1) \tag{20}$$

Finally, the de-convolution relationship between $I(t)$ and $\Phi(t)$ is described in Eq. (21). After substituting the detected current into Eq. (21) and combining with all the equations above, the modified neutron flux can be obtained.

$$\Phi'(n+1) = \frac{1}{S_{59}+S_{60}}[I'(n+1) - I'_{61}(n+1) - k_{60}\lambda_{60}N_{60}] \tag{21}$$

This model can not only solve the influence of background current which is generated by the Co SPND's material consumption, but also optimize the problem of delay current. The modified neutron flux can reflect the variation of the actual neutron flux realistically.

2.4. Other conditions before performance analysis

Let the detector work from time 0, and the material consumption rate η at time t can be expressed as Eq. (22). In which, $N_{59}(t)$ can be obtained by Eq. (4) and $\Phi(t)$ can be obtained by the measurement results before time t.

$$\eta = \frac{\int_0^t \sigma_{59}N_{59}(t)\Phi(t)dt}{N_{59}(0)} \tag{22}$$

Besides, in order to test and verify the performance of this model, step signal of neutron flux is taken as an example to analyze it. For step signal arrived at the moment t_0, the neutron flux can be written in Eq. (23).

$$\Phi(t) = \begin{cases} \Phi_0(t \geq t_0) \\ 0(t < t_0) \end{cases} \tag{23}$$

By substituting this step signal of neutron flux into Eq. (8), the theoretical current can be obtained as follow.

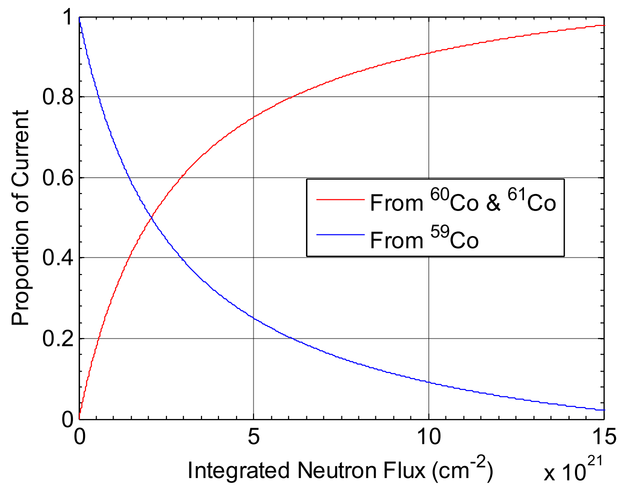

Fig. 2. The proportion of currents vary with integrated neutron flux when neutron flux is 10^{13} cm^{-2} s^{-1}.

$$I(t) = \Phi_0\{S_{59} + S_{60} + k_{61}\sigma_{60}N_{60}[1 - e^{-\lambda_{61}(t-t_0)}]\} + k_{60}\lambda_{60}N_{60} \tag{24}$$

When Co SPND is a new detector, the value of N_{59} is 9.081×10^{22} cm^{-3} and the value of N_{60} is 0 cm^{-3}. The other parameters are assumed as follows [16].

$S_{59} = 8.9527 \times 10^{-44} \times N_{59}$ A cm^2 s;
$S_{60} = 4.8172 \times 10^{-45} \times N_{60}$ A cm^2 s;
$k_{60} = 1.515 \times 10^{-21}$ A cm^3 s
$k_{61} = 1.5144 \times 10^{-20}$ A cm^3 s

3. Performance analysis of de-convolution model

3.1. The influence of material consumption and its compensation process

Generally, the delay time is the time it takes for the step signal to reach steady state. But in the next discussion, the delay time is defined as the time it takes for the step signal to reach 99% of the stability state. And in the following simulation, the value of sampling interval is supposed to be 0.001 s and the original current is overlaid with noise (Signal to noise ratio is 1000). For convenience, the start time of step signal is set to 1000 s. Before compensation, the moving-average filter (The filter order is 9) is used to reduce the impact of noise [17].

As the usage of Co SPND, more and more ^{60}Co nucleus are produced which causes the material consumption cannot be ignored. When the neutron flux is 10^{13} cm^{-2} s^{-1}, the circumstances of currents are shown in Fig. 2. The proportion of current generated by ^{59}Co is decreasing with the increase of integrated neutron flux, while the proportion of current generated by ^{60}Co and ^{61}Co is increasing with the increase of integrated neutron flux. It results in that higher and higher proportion of background current and delayed current appears with the increase of integrated neutron flux, leading to larger measurement error.

To eliminate the impact of material consumption, a modified model is established in section 2.3. It is taken as an example to analyze the performance of this model that the material consumption of Co SPND is 10%. The simulation results are shown in Fig. 3. Obviously, after the step signal of neutron flux arriving at the detector, the ideal current should be a constant and be proportional to neutron flux. But in fact, from Fig. 3, it shows that the theoretical detected current is not only out of proportion to neutron flux, but also varying with time. It takes more than 3070 s to achieve 99% of the stability state. Before compensation, the contribution of background current is more than 42%, which leads to a large measurement error. Therefore, it cannot reflect the variation of the actual neutron flux. However, after compensation, the background current and delayed current are removed, and the current can be proportional to neutron flux. Its delay time is just 0.004 s which is short enough to reflect the change of neutron flux in real time.

When the material consumption of Co SPND is 10%, the uncompensated currents in different neutron flux are shown in Fig. 4. The larger neutron flux is, the smaller the proportion of current produced by Co SPND's material consumption will be. It results in that the currents are nonlinear to neutron flux in the same material consumption of Co SPND. However, after compensation, the currents in different neutron flux are shown in Fig. 5. The background current and delayed current are removed. The proportion of each component of prompt currents does not vary with neutron flux. Therefore, the compensated currents can be linear to neutron flux.

3.2. Analysis of influencing factors

Due to the moving-average filter (The filter order is 9) is used in the compensation process to decrease the influence of noise, the sampling interval becomes an important parameter which has a great impact on delay time. Under normal circumstances, the sampling interval is no more than 1 s. Therefore, the sampling interval varying from 10^{-5} s–1 s is taken as an example to analyze its

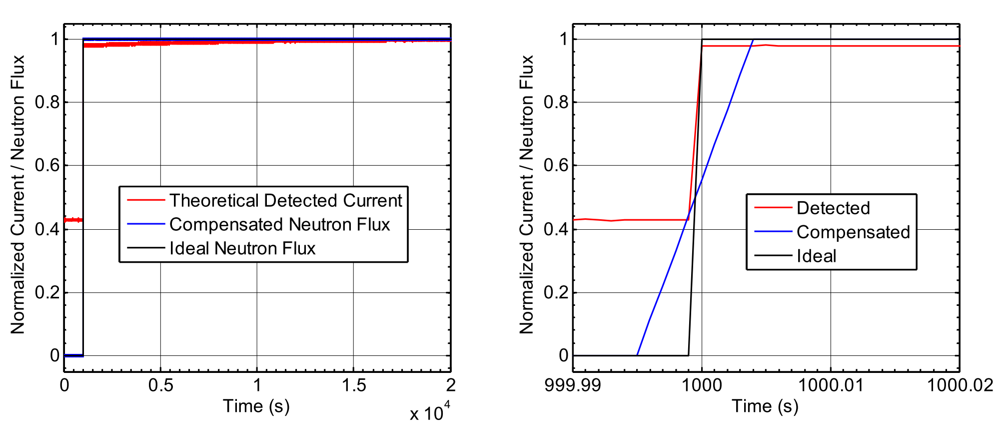

Fig. 3. The normalized current and neutron flux vary with time before and after compensation when the material consumption of Co SPND is 10%.

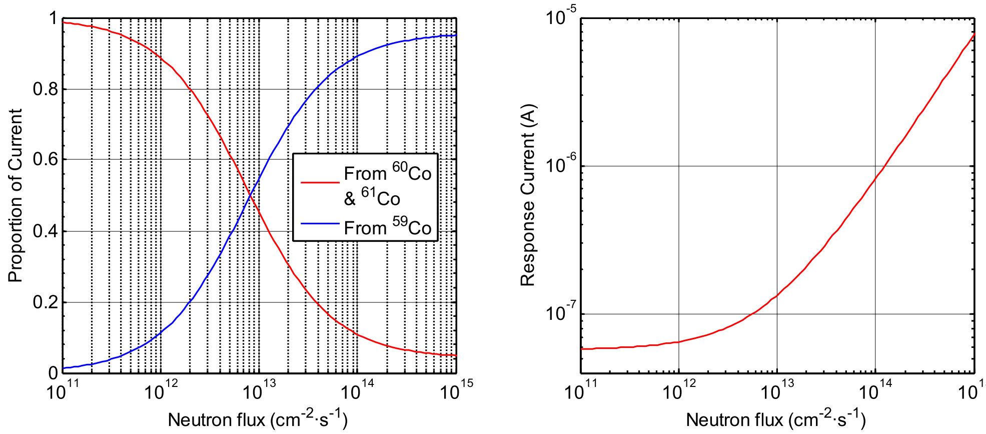

Fig. 4. The currents in different neutron flux before compensation when the material consumption of Co SPND is 10%.

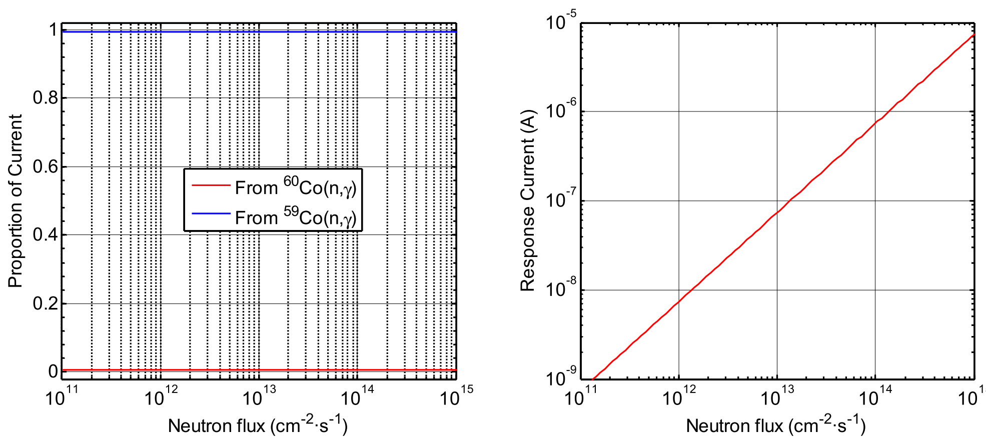

Fig. 5. The currents in different neutron flux after compensation when the material consumption of Co SPND is 10%.

influence. The simulation result is shown in Fig. 6. The delay time depends on the sampling interval and it is about four times of sampling interval in this compensation model. As long as the sampling interval is small enough, the real-time neutron flux can be obtained.

In order to test and verify the model's performance in the presence of noise, the delay time and normalized amplitude of fluctuation in different Signal to Noise Ratios (SNR) are obtained in Fig. 7. When the Signal to Noise Ratios is less than 100, the fluctuation of delay time appears which is caused by the fluctuation of amplitude. When the Signal to Noise Ratios is more than 100, the delay time remains unchanged at the value of 0.004 s. Therefore, the delay time has a good stability to noise as long as the signal-to-noise ratio is not too small.

In the simulation above, σ is considered to be the microscopic absorption cross section of thermal neutron. Due to the discussion is mainly based on the fast neutron flux environment, a suitable neutron moderation layer should be added around the detector according to the energy spectrum of neutron flux. This issue will be considered in future establishment of an experimental system. In addition, when Co SPND is used in thermal neutron flux environment, its performance is worse than Rh or V SPND, and a suitable current amplifier should be added in the external circuit to increase the current sensitivity.

Besides, in practical applications, parts of the detected currents are produced by other disturbance factors, such as gamma irradiation. In order to make the measurement results more accurate, another detector can be used as a reference object. The emitter of this detector uses materials with low neutron reaction cross section and its gamma reaction cross section is about the same with Co. This way, the impact of other factors can be greatly decreased.

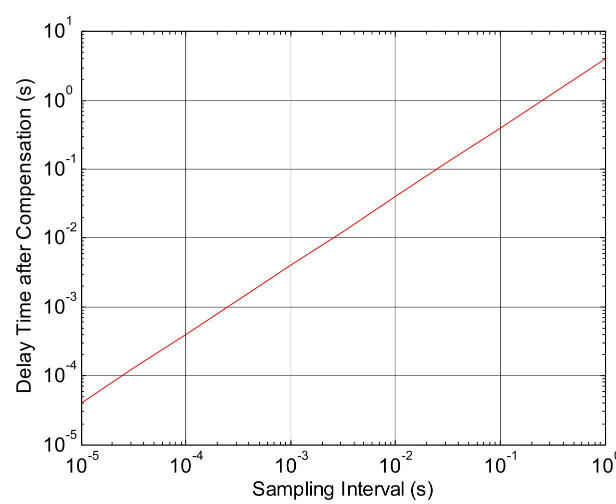

Fig. 6. The relationship between delay time and sampling interval when the material consumption of Co SPND is 10%.

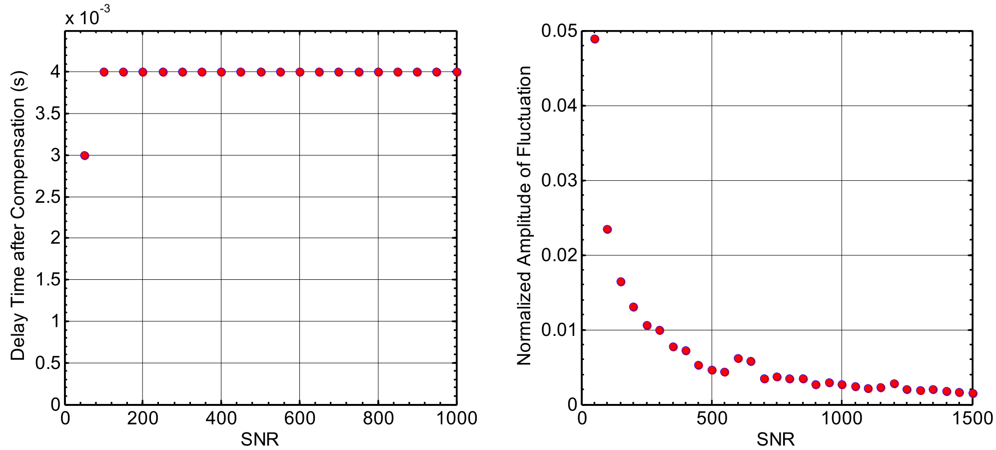

Fig. 7. The delay time and normalized amplitude of fluctuation in different Signal to Noise Ratios when the material consumption of Co SPND is 10%.

4. Conclusion

In order to solve the problems of background current and delayed current caused by the material consumption of Co SPND, a compensation model based on de-convolution method is established in this paper. Firstly, the current expression of Co SPND and the physical model of atomic density are established according to the physical principle of the interaction process. Then the unit impulse response of neutron flux $h(t)$ is obtained based on convolution method. Finally, by making use of discretization method and de-convolution method, the compensation relationship between $I(t)$ and $\Phi(t)$ can be inferred.

To test the performance of this compensation model, the compensated neutron flux is compared with the theoretical detected current and the ideal neutron flux when the material consumption of Co SPND is 10%. When the sampling interval is 0.001 s, the delay time of compensated neutron flux is only 0.004 s in comparison with the ideal neutron flux. After compensation, the background current and delayed current are eliminated. The compensated current is in correspondence of neutron flux, and it shows great improvement of performance relative to the theoretical detected current which is non-proportional to the neutron flux.

At last, the stabilities in different sampling intervals and different Signal-to Noise Ratios are analyzed. The delay time is about four times of sampling interval. If the sampling interval is small enough, the modified current can really reflect the change of neutron flux in real time. Besides, this method also has a good stability to noise.

This method can solve the influence caused by the material consumption of Co SPND, which provides great help to the design of Co SPND's detection system.

Acknowledgement

Thanks for permission to publish this paper by National University of Defense Technology.

Appendix A. Supplementary data

Supplementary data to this article can be found online at https://doi.org/10.1016/j.net.2019.09.010.

References

[1] W.H. Todt, Characteristics of self-powered neutron detectors used in power reactors, in: In-Core Instrumentation and Core Assessment, Proceedings of a Specialists' Meeting, Mito-shi, Japan, 1996.
[2] Q. Zhang, X. Liu, B. Deng, et al., Numerical optimization of rhodium self-powered neutron detector, Ann. Nucl. Energy 113 (2018) 519–525.
[3] R. Van Nieuwenhove, Effect of fission betas, activated structures and hydrogen on self powered neutron detectors, IEEE Trans. Nucl. Sci. 61 (4) (2013) 2006–2010.
[4] A.K. Mishra, S.R. Shimjith, T.U. Bhatt, et al., Dynamic compensation of vanadium self powered neutron detectors for use in reactor control, IEEE Trans. Nucl. Sci. 60 (1) (2013) 310–318.
[5] P.S. Rao, A.K. Mahant, S. Rao, et al., Some studies on cobalt and vanadium self powered neutron detectors developed by ECIL, Radiat. Phys. Chem. 51 (4–6) (1998) 453–454.
[6] K. Srinivasarengan, L. Mutyam, M.N. Belur, et al., Flux estimation from vanadium and cobalt self powered neutron detectors (SPNDs): nonlinear exact inversion and kalman filter approaches, in: American Control Conference, IEEE, 2012, pp. 318–323.
[7] M. Alex, M.D. Ghodgaonkar, Development of an inconel self-powered neutron detector for in-core reactor monitoring, Nucl. Instrum. Methods Phys. Res. Sect. A Accel. Spectrom. Detect. Assoc. Equip. A 574 (1) (2007) 127–132.
[8] D. Bi, D. Xu, J. Bu, A unified framework for modeling slow response self-powered neutron detectors with discrete-time state-space representation, in: International Conference on Advancements in Nuclear Instrumentation Measurement Methods and Their Applications, 2014, pp. 1–5.
[9] X. Peng, Q. Li, W. Zhao, et al., Robust filtering for dynamic compensation of self-powered neutron detectors, Nucl. Eng. Des. 280 (2014) 122–129.
[10] A.K. Mishra, S.R. Shimjith, T.U. Bhatt, et al., Kalman filter-based dynamic compensator for vanadium self powered neutron detectors, IEEE Trans. Nucl. Sci. 61 (2014).
[11] Q. Zhang, B. Deng, X. Liu, et al., Deconvolution-based real-time neutron flux reconstruction for self-powered neutron detector, Nucl. Eng. Des. 326 (2018) 261–267.
[12] H. Lee, S. Choi, K.H. Cha, et al., New calculational model for self-powered neutron detector based on Monte Carlo simulation, J. Nucl. Sci. Technol. 52 (5) (2015) 660–669.
[13] N.P. Goldstein, A Monte-Carlo calculation of the neutron sensitivity of self-powered detectors, IEEE Trans. Nucl. Sci. 20 (1973) 549–556.
[14] W. Lee, G. Cho, K. Kim, et al., A study on the sensitivity of self-powered neutron detectors (SPNDs), IEEE Trans. Nucl. Sci. 48 (4) (2001) 1587–1591.
[15] Wolfgang Wiesenack, Comment on "Vanadium, rhodium, silver and cobalt self-powered neutron detector calculations by RAST-K v2.0", Ann. Nucl. Energy 115 (2018) 633–634.
[16] R.A. Razak, M. Bhushan, M.N. Belur, et al., Clustering of self powered neutron detectors: combining prompt and slow dynamics, IEEE Trans. Nucl. Sci. 61 (6) (2014) 3635–3643.
[17] K. Mivule, C. Turner, Applying moving average filtering for non-interactive differential privacy settings, Procedia Comput. Sci. 36 (6) (2014) 409–415.